MODELING AND CHARACTERIZATION OF MULTIPLE LEVEL INTERMEDIATE BAND SOLAR CELL

P. G. Linares*, A. Martí, E. Antolín, E. Hernández, I. Ramiro and A. Luque
Instituto de Energía Solar, Universidad Politécnica de Madrid, 28040 Madrid, Spain
Phone: +34 914533549 FAX: +34 915446341 email: p.garcia-linares@ies-def.upm.es

C. D. Farmer and C. R. Stanley
Department of Electronics and Electrical Engineering, Univ. of Glasgow, Glasgow G12 8QQ, U.K.

ABSTRACT: Intermediate band solar cells (IBSCs) are a new kind of devices capable of surpassing the Shockley-Queisser efficiency limit for conventional solar cells. This novel technology requires the use of a new type of material named intermediate band (IB) material which makes a better use of the solar spectrum thanks to the existence of a collection of electronic levels within the bandgap of the semiconductor. Quantum Dots (QDs) remain as a feasible technology to implement IB materials. InAs/GaAs QD-IBSCs were manufactured in order to test the validity of the concept, although their real size and shape are far from the optimum. This causes extra electron levels to appear within the nanostructure confining potential, degrading the performance of the device. In this paper, the effect of these extra levels will be studied through a multiple level IBSC model based on the detailed balance, but modified so a term accounting for the non-radiative recombination (NRR) is also included. The model is completed with constant fitting parameters so the concentration J_L-V_{OC} curves (which do not incorporate series resistance effects) can be fitted. Several QD-IBSCs where manufactured, measured and fitted with this model, rendering relevant information about the recombination nature of the QD-IBSCs.

1 INTRODUCTION

The IBSC is a Photovoltaic concept proposed in 1997 as a way to exceed the Shockley-Queisser limit [1]. Limiting efficiencies above 63% are calculated for such novel concept in comparison to the 41% efficiency limit of the single junction solar cell (SC). The IBSC is based on a material hosting a collection of levels within the bandgap forming a band (the IB) well separated from both the conduction band (CB) and the valence band (VB). The latter allows three different possible groups of transitions [2] (all illustrated in Fig. 1): from the VB to the CB (labeled as g_{CV}), from the VB to the IB (labeled as g_{IV}), and from the IB to the CB (labeled as g_{CI}). Therefore, apart from the usual transition g_{CV}, electrons can be promoted to the CB through a two step process using the IB as an intermediate step. Furthermore, if the IB is isolated from the contacts, the open circuit voltage (V_{OC}) of the IB will be only limited by the host material bandgap (E_G in Fig. 1) and not by any of the sub-bandgaps (E_H or E_L in Fig 1). Thanks to this last feature, the IBSC provides additional current without limiting the potential of achieving a high V_{OC}, which explains the extra efficiency predicted by these devices.

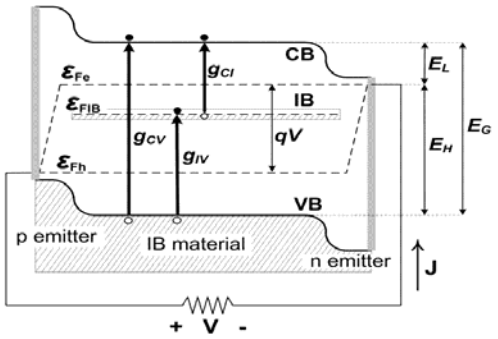

Figure 1: Schematic of the band diagram of an IBSC where all different transitions are represented. The quasi-Fermi levels (QFLs) ε_{Fe}, ε_{Fh} and ε_{FIB} corresponding to each of the electron gases are also defined in the figure.

The IBSC can be implemented with QDs, which allow discrete electron confined levels that can act as the IB. An IBSC was first manufactured including several stacked InAs QD layers and GaAs as the barrier material, all embedded in GaAs emitters [3] (in order to isolate the IB from the contacts). The operational principles of the IBSC were satisfactory tested [4], although the efficiency boost was not achieved.

Far from the idealized behavior, the aforementioned QD system allows more than one confined state that can be detrimental for the electrical performance of the SC. Furthermore, several confined states have been identified in the QDs that have been inserted in the QD-IBSCs [5].

This work presents an alternative model for the analysis of IBSCs implemented with QDs, accounting for the more realistic multiple level case. The model, which was first presented in Ref. [6], is used to analyze SCs through modified detailed balance calculations combined with experimental J_L-V_{OC}, which render valuable information on the performance of the different transitions occurring at the QD-IBSC.

2 THE MULTIPLE LEVEL IBSC

Fig. 2(a) shows a simplified sketch of the three bands present in an IBSC (the IB being multilevel). Each arrow represents the possible transitions occurring from the VB to the CB or to any of the IB levels (first step of the sub-bandgap generation and recombination processes) and also the ones from the IB levels to the CB (second step of the same processes). E_V represents the top of the effective VB and E_C the bottom of the effective CB. E_{ti} (i =1, 2, 3, and 4) represents the energy of the IB levels. Although there are many confined hole levels in the VB offset, they do not produce any transition in our model because they are located very close to each other and thus, E_V represents the uppermost of the VB. E_C represents, more precisely, the energy of the confined states of the wetting layer (WL), which is a quantum well produced by the Stranski-Krastanov growth mode [7]. Both the confined hole levels and the WL reduce the

main bandgap width, which is why the CB and VB are referred as "effective".

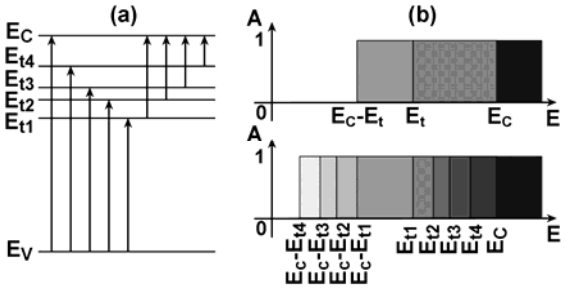

Figure 2: (a) Schematic of all possible transitions involving the three existing bands (VB, IB and CB) that have been considered in our model. (b) Absorption diagram for the single and the multiple level cases, where the energy of each absorption threshold is shown in accordance with the energy of each of the intermediate levels.

The lower part of Fig. 2(b) is a representation of the energy intervals producing the transitions which have been already mentioned. The previous constitute the integration intervals used in our modified detailed balance model. The upper part of the figure represents the energy intervals of the single level IBSC case, where E_t is the energy of the IB. Table 1 shows the energy (in eV) of each of the four confined electron levels (E_{ti}), as well as the effective VB and CB (E_C and E_V). Four main electron confined levels were identified thanks to the internal quantum efficiency experiments carried out on the three IBSCs that have been analyzed in this work (denoted as Sample A, B and C).

Table I: energy of the four levels identified in each of the three QD-IBSCs samples studied in this work

Energy level\Sample	A	B	C
E_C	1.35	1.21	1.21
E_{t4}	1.225	1.144	1.18
E_{t3}	1.175	1.105	1.14
E_{t2}	1.137	1.015	1.075
E_{t1}	1.052	0.953	0.974
E_V*	0	0	0

*The effective top of the VB is considered as the zero potential energy of the system.

Fig. 3 represents the generalized equivalent circuit for the multiple level IBSC. On the left part of the figure, the host subcell set consisting on a photocurrent generator in parallel with a diode can be found. They represent the VB→CB pumping and recombination respectively. In parallel with this host subcell, we can find a series combination of two other subcells, representing the VB→IB and IB→CB transitions. There are four of these secondary subcell sets representing pumping and recombination through each of the four confined levels (termed IBs).

In our detailed balance analysis, no transition can occur among the different confined levels. The reason arises from the fact that these levels are regarded as fine lines (δ functions in energy) and therefore, the associated energy interval for integration is zero. However, non-radiative transitions among confined levels are possible (and very likely because of their proximity) and enhance the electron transfer between the different levels of the multiple level IBSC. The limit is the case where the different IB levels are short-circuited, which would be equivalent to connect the points I1, I2, I3 and I4 in Fig 3. The latter implies that the four levels share a single quasi-Fermi level (QFL) and in the following corresponds to the case of study named as "connected", which will have its own mathematical model for the possible fitting of the measured samples.

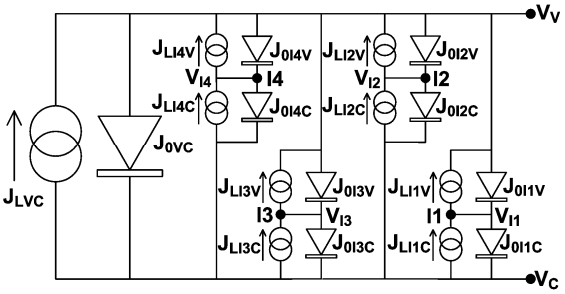

Figure 3: Equivalent circuit for a four-level IBSC. The voltages correspond to the QFL at the different energy levels or bands.

The recombination term used in our theoretical model is based on the Roosbroeck-Shockley formula [8] shown in Ec. (1).

$$J_{thr}(E_m, E_M) = \frac{2\pi}{h^2 c^3} \int_{E_m}^{E_M} E^2 \exp\left[-(E - F_t)/kT\right] dE \quad (1)$$

In this formula, F_t represents the IB QFL located at the level E_t and T is the cell temperature. The model is parameterized with constants that multiply each of the recombination terms associated to the different transitions, so we can obtain the appropriated fitting of the J_L-V_{OC} measurement of the cells. These J_L-V_{OC} pairs are obtained under different levels of concentrated light and the reason for it is that this measurement reproduces the dark *J-V* curve of the SC without the series resistance component.

The set-up shown in Fig. 4 is used for the acquisition of the concentrated light *J-V* points, which are measured at room temperatures (T=298K). The set-up is based on a flash light together with a concentration lens (see Fig. 4) with which the concentration level can reach as high as 10,000 suns. The system also integrates a very fast data acquisition system and a four-quadrant voltage source used at four-wire measuring mode. The sample is stabilized at the desired temperature thanks to a thermoelectric Peltier device.

The constants parameterizing the different recombination terms in our model constitute the central point of our analysis. F_{CV} is the parameter associated to the recombination at the fundamental transition (VB→CB) and F_{Ci} and F_{Vi} (i =1, 2, 3 and 4) are the parameters associated to the VB→IB and IB→CB

transitions respectively. All of the previous correspond to the radiative and NRR (this last case associated to the parameters greater than 1) in the neutral zones (m=1). However, to properly account for the recombination taking place on the space charge region (m=2), another term proportional to exp($eV/2kT$) has been included in our model. F2 is the fitting parameter associated to it.

The VB→IB and IB→CB recombination terms accounted in the connected model (where a single QFL describes the carrier population in all the IB levels) are calculated as the sum of the recombination terms corresponding to the different transitions from the VB to each of the IB levels and from each of the IB levels to the CB respectively. The fitting parameters associated to the aforementioned recombination terms are denoted as F_{VT} and F_{CT}.

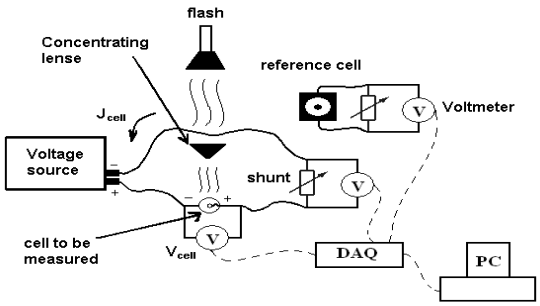

Figure 4: Representation of the concentration set-up used for the acquisition of the J_L-V_{OC} measurements. The sample temperature is stabilized by a Peltier cell.

3 RESULTS

Three QD-IBSCs have been manufactured with different QD technologies. Then, their J_L-V_{OC} characteristic have been measured under concentration and they have been fitted with the aforementioned model, either with the "connected" or with the "disconnected" approximation.

Fig. 5 shows the J_L-V_{OC} measurements (up to 10,000 suns) of the GaAs reference cell and the three QD samples. Each of the QD samples has been manufactured with a different technological approach. The SC denoted as sample A and shown in Fig. 5(b) was manufactured with ten stacked InAs/GaAs QD layers inserted between the GaAs emitters. The QDs in this sample are relatively small, the stacks are separated by thin spacers and the SC layer structure is simple. Sample B in Fig. 5(c) is different from sample A because a quaternary AlGaInAs layer [9,10] and a QD seed layer have been introduced in the cell structure with the purpose of enhancing the QD size. It also has other different technological features like the inclusion of field damping layers [11]. Sample C in Fig. 5(d) is similar to sample B except for having a thinner n-doped base, larger spacers and also for hosting thirty QD layers, instead of ten.

The fitting of the GaAs reference cell shown in Fig. 5(a) reveals a J_{0CV} 150 times the Roosbroeck-Shockley term (F_{CV}=150). This means that the total recombination in our cell is 150 times the minimum theoretical value (radiative limit) in the case of a simple GaAs technology. This value can be seen as the baseline for comparison with the QD-IBSC prototypes. $F2$=0.13, which has no physical meaning, except for giving an idea of the magnitude of the NRR as a threshold for the analysis of further QD SCs. Sample A can only be fitted through the connected level model (single QFL) with the following parameters: F_{CV}=27,000, which implies a considerably high deterioration of the host subcell; $F2$=2.8, meaning that the introduction of the QDs has severely increased the non radiative recombination in the space charge region; F_{VT}=12 and F_{CT}=2 which are the parameters multiplying the Roosbroeck-Shockley term for the combined effect of the recombination (corresponding to VB→IB and IB→CB, respectively) over the four IB levels of this single QFL model.

Samples B and C require the disconnected level model (four independent QFLs) in order to be correctly fitted. This is probably related to the fact that both samples have their tunnel carrier escape mechanism inhibited [10,12], compared to sample A, and therefore, each of the different IB levels can be defined by its own independent carrier population.

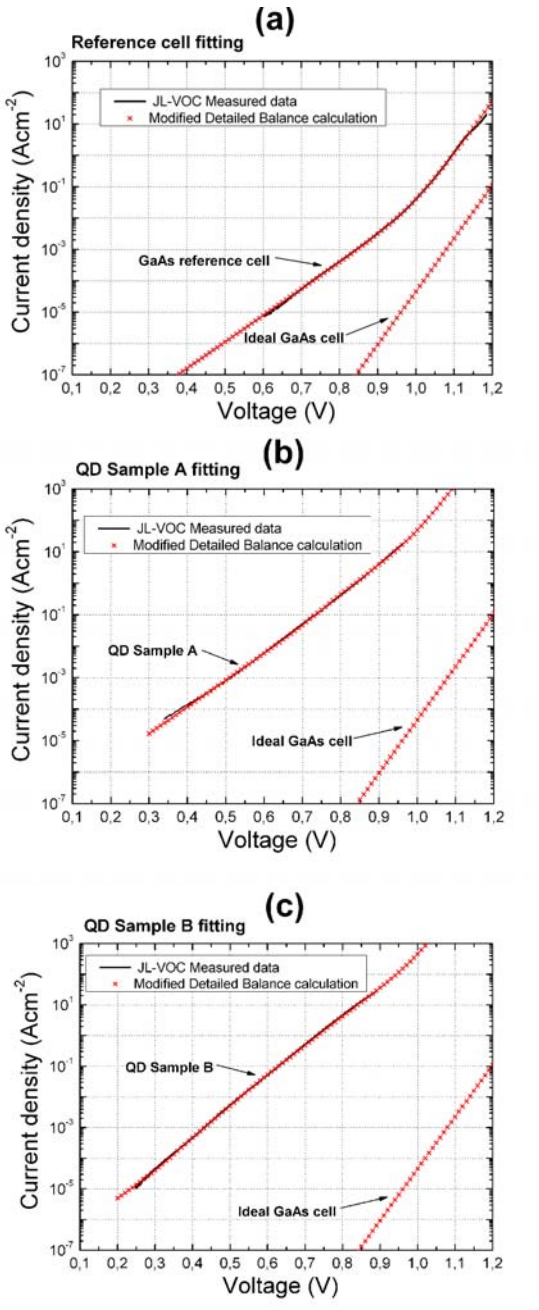

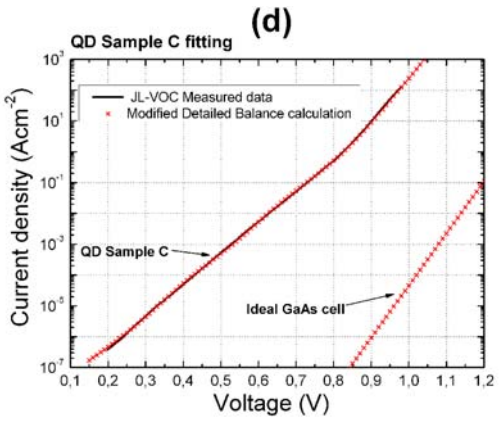

Figure 5: Representation of the concentration J_L-V_{OC} measurements and fittings of different QD-IBSC samples, together with a GaAs reference cell. All the previous plots are compared with the ideal GaAs cell. (a) J_L-V_{OC} and fitting of the GaAs reference SC; (b) J_L-V_{OC} and fitting of sample.A; (c) J_L-V_{OC} and fitting of sample.B; (c) J_L-V_{OC} and fitting of sample.C.

The following Roosbroeck-Shockley parameters are characteristic for sample B: F_{CV}=1,400; $F2$=1.8; F_{V1}=2,000; F_{V2}=1,300; F_{V3}=1,300; F_{V4}=0.01; F_{C1}=0.3; F_{C2}=2; F_{C3}=6; F_{C4}=0.01. And these other factors typically fit sample C with the same applied model: F_{CV}=950; $F2$=0.2; F_{V1}=850; F_{V2}=600; F_{V3}=400; F_{V4}=400; F_{C1}=0.01; F_{C2}=0.15; F_{C3}=0.01; F_{C4}=200.

It is important to remark that a low Roosbroeck-Shockley factor does not necessary imply a strong radiative behavior of the transition, since it can also be related to a poor absorption [13]. This is because the detailed balance model assumes total absorption of the incoming photons and therefore, even in the radiative limit, the associated parameter of a transition may be below one (although it may seem against intuition).

All the data presented here constitute an important source of information on the nature of the transitions involved in the IBSC (generalized to the multiple level case), not only concerning the strength of their radiative character.

4 CONCLUSIONS

A model to evaluate the different recombination components for the multiple level IBSC has been used to characterize the performance of three different QD-IBSCs, which were compared to a GaAs reference cell.

Besides providing fruitful information on the nature and magnitude of the recombination between the different transitions, the fittings reveal whether the different levels of the IBSC are connected or not.

The model constitutes a valuable tool for the characterization of the future IBSCs.

ACKNOWLEDGEMENTS

This work has been supported by the IBPOWER project funded by the European Commission (Grant Agreement No. 211640) and by the Spanish National Research Programs DenQuIBand (Grant Agreement No. PLE2009-0045) and NANOGEFES (Grant Agreement No. ENE2009-14481-C02-02).

REFERENCES

[1] A. Luque and A. Martí, Phys. Rev. Lett. **78**, pp. 5014 (1997).

[2] A. Martí, L. Cuadra and A. Luque, NEXT GENERATION PHOTOVOLTAICS: High Efficiency through Full Spectrum Utilization, A. Martí and A. Luque, Eds. Bristol: Institute of Physics Publishing (2003).

[3] A. Luque, A. Martí, C. Stanley, N. López, L. Cuadra, D. Zhou, and A. Mc-Kee, J. Appl. Phys., vol. **96**, no. 1, pp. 903–909 (2004).

[4] A. Martí, E. Antolín C. R. Stanley, C. D. Farmer, N. López, P. Díaz, E. Cánovas, P. G. Linares, and A. Luque, Phys. Rev. Lett. **94**, pp. 247701 (2006).

[5] E. Cánovas, A. Martí, N. López, E. Antolín, P. G. Linares, C. D. Farmer, C. R. Stanley, and A. Luque, Thin Solid Films **516**, 6943 (2008).

[6] A. Luque, P.G. Linares, E. Antolín, E. Cánovas, C.D. Farmer, C.R. Stanley, and A. Martí, Appl. Phys. Lett. **96**, 013501 (2010).

[7] M.Sugawara, "Self-assembled InGaAs/GaAs quantum dots", Vol. 60: Academic Press, New York (1999).

[8] W. van Roosbroeck and W. Shockley, Phys. Rev. **94**, 1558 (1954).

[9] P.G.Linares, C.D. Farmer, E. Antolín, S. Chakrabarti, A.M. Sánchez, T. Ben, S.I. Molina, C.R. Stanley, A. Martí, A. Luque, Energy Procedia **2**, 133–141 (2010).

[10] E. Antolín, A. Martí, C.D. Farmer, P. G. Linares, E. Hernández, A.M. Sánchez, T. Ben, S.I. Molina, C.R. Stanley, A. Luque, J. of Appl. Phys (2010), *in press*.

[11] A. Martí, E. Antolín, E. Cánovas, N. López, P.G. Linares, A. Luque, C.R. Stanley, C.D. Farmer, Thin Solid Films **516**, 6716–6722 (2008).

[12] E. Antolín, A. Martí, P.G. Linares, I. Ramiro, E. Hernández, C.D. Farmer, C.R. Stanley, and A. Luque, in Proc. of the 35th IEEE Photovoltaic Specialists Conference, Hawaii (2010).

[13] A. Luque, A. Martí, E. Antolín, and P. G. Linares, Sol. Energy Mat. Sol. Cells (2010), *in press*.